

## Point-spread function in depleted and partially depleted CCDs

D. E. Groom,<sup>1</sup> P. H. Eberhard, S. E. Holland, M. E. Levi,  
N. P. Palaio, S. Perlmutter

*Lawrence Berkeley National Laboratory, Berkeley, CA 94720*

and

R. J. Stover, M. Wei

*University of California Observatories/Lick Observatory*

*University of California, Santa Cruz, CA 95064*

### ABSTRACT

The point spread function obtainable in an astronomical instrument using CCD readout is limited by a number of factors, among them the lateral diffusion of charge before it is collected in the potential wells. We study this problem both theoretically and experimentally, with emphasis on the thick CCDs on high-resistivity n-type substrates being developed at Lawrence Berkeley National Lab.

*Subject headings:* CCD, high resistivity, fully depleted, astronomical, Lick Observatory, Lawrence Berkeley National Laboratory

### 1. Introduction

CCD image sensors of novel design for applications in astronomy are being developed and tested at Lawrence Berkeley National Lab (LBNL) and Lick Observatory (UCO/Lick) (Holland et al. 1996; Stover et al. 1999). The devices are fabricated on high-resistivity, n-type substrates and are back illuminated. In normal operation, a substrate bias voltage applied to the back-side contact results in full depletion of the 300  $\mu\text{m}$  thick substrate. This is in contrast to previous deep-depletion CCDs with typically 50  $\mu\text{m}$  thick depletion regions (Burke et al. 1997, 1994, 1991; Kamasz et al. 1994; Tsoi et al. 1985). The depletion voltage is relatively low ( $\lesssim 20$  V) due to the high resistivity of the starting silicon ( $\approx 10,000$   $\Omega\text{-cm}$  which corresponds to a substrate doping density  $N_D$  in the mid- $10^{11}$   $\text{cm}^{-3}$  range).

A concern for such CCDs is spreading via dif-

fusion of the photogenerated charge during the transit from the back side of the device, where short-wavelength light is absorbed, to the CCD potential wells located nearly 300  $\mu\text{m}$  away. In this paper we extend the theoretical analysis of an earlier study (Holland et al. 1997) of the charge spreading issue, and present new measurements, obtained with a pinhole mask in contact with a  $2048 \times 2048$  (15  $\mu\text{m}$ )<sup>2</sup> pixel back-illuminated device. Exposures to blue light were made at different bias voltages. While voltages too low for total depletion are not recommended for normal operation, data obtained under such conditions yields useful model parameters.

### 2. One-dimensional approximation

We consider the electric fields in a partially- or fully-depleted CCD fabricated on a high-resistivity n-type substrate. Except near the gate structure (on the scale of a pixel width) the electric field in the substrate can be regarded as a function

---

<sup>1</sup>DEGroom@lbl.gov

of  $z$  alone, where  $z$  is the coordinate normal to the plane of the CCD. The field distribution can be obtained from the analysis of a simple overdepleted CCD structure, as was done by Holland et al. (1997), who obtained

$$E(z) = E_{\min} + \frac{qN_D}{\epsilon_{\text{Si}}} z, \quad (1)$$

where the electric field at  $z = 0$  is given by

$$E_{\min} = \left( \frac{V_{\text{sub}} - V_J}{z_J} - \frac{1}{2} \frac{qN_D}{\epsilon_{\text{Si}}} z_J \right). \quad (2)$$

We have chosen to measure  $z$  from the back surface of the CCD to expedite diffusion calculations, although the choice is inappropriate for potential calculations. Here  $q$  is the electronic charge,  $N_D$  is the donor atom density in the depleted region, and  $\epsilon_{\text{Si}}$  is the permittivity of silicon (about  $11.7\epsilon_0$ ).  $V_{\text{sub}}$  is the substrate bias voltage, and  $V_J$  is essentially the voltage at the p-n junction, at  $z = z_J$ . The voltage drop across the drift region,  $V_{\text{sub}} - V_J$ , is assumed to be larger than the depletion voltage,  $qN_D z_J^2 / 2\epsilon_{\text{Si}}$ .

If this is not the case,

$$E(z) = \begin{cases} (qN_D/\epsilon_{\text{Si}})(z - z_{ff}) & \text{if } z > z_{ff} \\ 0 & \text{otherwise.} \end{cases} \quad (3)$$

The boundary between the field-free and depleted regions is at  $z = z_{ff}$  and is obtained from the condition  $E(z_{ff}) = 0$ , which yields

$$z_J - z_{ff} = \sqrt{(2\epsilon_{\text{Si}}/qN_D)(V_{\text{sub}} - V_J)} \quad (4)$$

for the thickness of the depletion region. For the special case  $z_{ff} = 0$  (barely depleted), it can be checked that Eq. 4 implies  $E_{\min} = 0$  in Eq. 2. These fields are sketched in Figure 1.

Equations 1–4 were derived from a one-dimensional analysis. For CCDs on high-resistivity silicon the potentials are strongly two-dimensional (Burke et al. 1994; McCann et al. 1980). A region exists below the buried channel implant where the field is significantly larger than  $E(z_J)$  given by Eq. 1. Figure 2 shows a two-dimensional simulation of one pixel of a high-resistivity CCD. As shown, the potential varies strongly under the collection electrode, and the field at  $z_J$  is much greater than predicted by Eq. 1. As a practical matter, charge spreading in the high-field region is negligible and Eqs. 1 and 2 can still be used,

but  $V_J$  is not the potential at the junction but at the point where the field deviates from Eq. 1. According to this analysis, the thickness of the drift region will be less than  $z_J$  by about 5–10  $\mu\text{m}$ . These quantities are distinguished by primes in Figure 2, but the distinction will be dropped in the following sections.

### 3. Continuity equation

For a p-channel device in which recombination is unimportant, the hole density is given by

$$D_p \nabla^2 p - \mu_p \nabla(p\mathbf{E}) + G_p = \frac{\partial p}{\partial t}, \quad (5)$$

where  $D_p$  and  $\mu_p$  are the hole diffusion constant and mobility and  $G_p$  is the hole generation rate (Shockley 1950). In the following discussion the Einstein relation  $D_p/\mu_p = kT/q$  is occasionally employed.

For our present purposes we take  $G_p = \delta(x)\delta(y)\delta(z)\delta(t)$ , that is, a point source of blue light at  $t = 0$ .<sup>2,3</sup> Then everywhere but at the  $\delta$ -function source, and with  $\mathbf{E} = (0, 0, E(z))$ , we have

$$D_p \nabla^2 p - \mu_p \frac{\partial}{\partial z}(p E_z) \equiv -\nabla \mathbf{j} = \frac{\partial p}{\partial t}, \quad (6)$$

where we find it convenient to define the probability current density  $\mathbf{j} = -D_p \nabla p + \mu_p p \mathbf{E}$ .<sup>4</sup>

Holes encountering the back surface of a fully-active CCD are diffusely reflected, and there is no current across the  $z = 0$  boundary:  $j_z(x, y, 0, t) = 0$ . At the junction near the potential wells ( $z = z_J$ ) the hole density vanishes:  $p(x, y, z_J, t) = 0$ .

It may be verified directly that the solution

$$p = \frac{1}{\sqrt{2\pi} 2D_p t} e^{-(x^2+y^2)/4D_p t} g(z, t) \quad (7)$$

satisfies the boundary conditions, with the ‘‘longitudinal function’’  $g(z, t)$  satisfying

$$\frac{\partial}{\partial z} \left( D_p \frac{\partial g}{\partial z} - g E(z) \right) = \frac{\partial g}{\partial t} \quad (8)$$

<sup>2</sup>It is not difficult to replace  $\delta(z)$  by  $\delta(z - z_s)$  and integrate over a distributed source distribution, as should be done for red light, but there is not enough room in the margin of this report.

<sup>3</sup>In practice photons produce electron/hole pairs ‘‘one at a time,’’ and space-charge effects are not important. We interpret  $p$  as the probability density function for the charge distribution.

<sup>4</sup>Multiply by  $q$  to get a conventional current density.

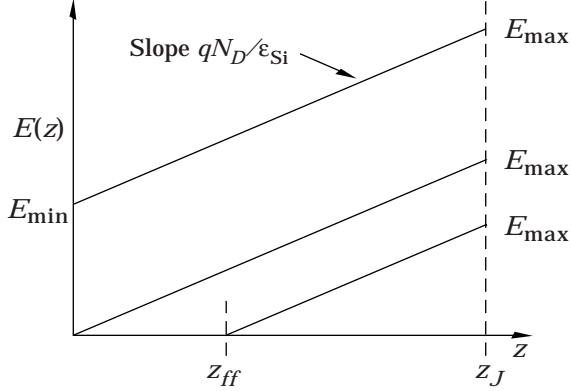


Fig. 1.— Electric fields in a thick CCD substrate for different back-surface bias potentials. In the underdepleted case the field is zero for  $z < z_{ff}$  and rises linearly with slope  $N_D/\epsilon_{Si}$  to  $E_{\max}$  at the p-n junction. If the bias potential is large enough the field starts at  $E_{\min} \geq 0$  at the back surface.

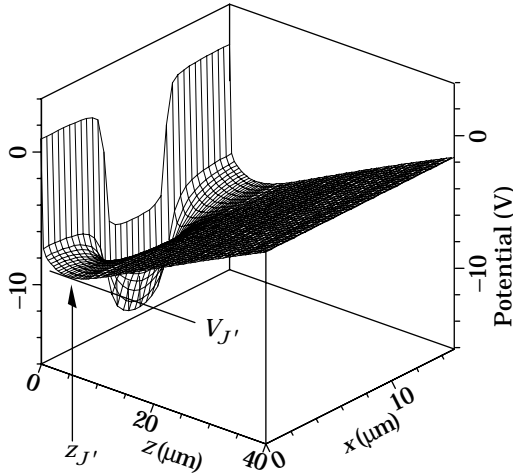


Fig. 2.— Simulated potential distribution for a  $15 \mu\text{m}$  pixel. The substrate doping was  $6 \times 10^{11} \text{ cm}^{-3}$  and the buried-channel implant dose was  $1.5 \times 10^{12} \text{ cm}^{-2}$ . WARNING: The labeled axis measure  $z$  from the front of the CCD, in distinction to practice elsewhere in this paper.

and the boundary conditions  $g(z_J, t) = 0$  and  $\partial g/\partial z|_{z=0} = 0$ .

We make a simple observation from Eq. 7 which will be used repeatedly in this paper:

*The charge being collected by the potential wells at a given time  $t$  has a Gaussian lateral distribution with standard deviation  $\sigma = \sqrt{2D_p t}$ .*

Our desired solution (the PSF) is the normal component of the probability current density at this surface,  $j_z(x, y, z_J, t) = -\partial p/\partial z|_{z_J}$ , integrated over time:

$$\begin{aligned} f(x, y) &= \int_0^\infty j_z(x, y, z_J, t) dt \\ &= \int_0^\infty -\frac{\partial g}{\partial z}\bigg|_{z=z_J} \frac{1}{2\pi 2D_p t} e^{-(x^2+y^2)/4D_p t} dt \end{aligned} \quad (9)$$

#### 4. Diffusion in a depleted CCD

We assume that the CCD is overdepleted, so that  $E_{\min} > 0$ , and temporarily neglect longitudinal diffusion. All charges then arrive at the same time, and hence distribute radially as a Gaussian according to Eq. 7. The mean transit time may be calculated by integrating  $dz/v(z)$ , where the drift velocity  $v(z)$  is  $\mu_p E(z)$  for electric fields below the velocity saturation limit. In the present case

$$v(z) = \mu_p \left( E_{\min} + \frac{qN_D}{\epsilon_{Si}} z \right), \quad (10)$$

from which we obtain the variance in  $x$  (or  $y$ ),

$$\sigma_d^2 = 2D_p t = 2 \frac{kT}{q} \frac{\epsilon_{Si}}{qN_D} \ln \frac{E_{\max}}{E_{\min}}. \quad (11)$$

At high fields  $E_{\min} \approx E_{\max}$ , and one may expand the above expression to obtain the asymptotic result

$$\sigma_{\text{asympt}}^2 = 2 \frac{kT}{q} \frac{z_J^2}{V_{\text{sub}} - V_J}. \quad (12)$$

From this we observe that in the overdepleted case the PSF width scales linearly with the wafer thickness, as the square root of temperature, and inversely as the square root of the applied voltage (very nearly the substrate voltage).

If the substrate is just barely depleted or underdepleted, then  $E_{\min} = 0$  and Eq. 11 is divergent. This is to be expected, since we have neglected

longitudinal diffusion. The charges are produced in a field-free region, and in this approximation take infinite time to get out. We will deal with this problem later.

But how serious is our neglect of longitudinal diffusion in the overdepleted case? An almost-solution provides insight. If  $E_z(z)$  is replaced by its average value  $E_c$  in Eq. 6, then a solution which satisfies the boundary condition at  $t = 0$  is

$$g(z, t) = \sqrt{\frac{1}{4\pi D_p t}} e^{-(z-v_c t)^2/4D_p t} \quad (13)$$

where  $v_c = \mu_p E_c$ . The boundary condition  $g(z_J, t) = 0$  is satisfied only for times sufficiently small that the tail of the distribution do not yet reach the boundary at  $z = z_J$ , i.e., roughly for  $t < z_J/v_c$ . The picture is simple: the  $\delta$ -function distribution at the back surface at  $t = 0$  grows into a Gaussian distribution in three dimensions, with  $\sigma = \sqrt{2D_p t}$ , whose centroid moves with velocity  $v_c$ . The expanding ball of charge reaches the potential wells over a fractional transit time  $\sigma_d/z_J$ . If this fraction is small compared with unity (as it turns out to be), then our Gaussian approximation for the lateral distribution is valid.

### 5. Resolution dominated by diffusion in a field-free region

At low bias voltages for the LBNL CCDs and nearly always for thinned CCDs, the substrate is not fully depleted. For most optical wavelengths and in particular for the blue, light is absorbed very close to the back surface, and carriers freely diffuse through the undepleted substrate until they cross the interface, encounter an electric field, and travel to the CCD potential wells. As mentioned above, recombination may be neglected for the cases being considered. We consider a point source of charge carriers at the rear surface of a CCD with a field-free thickness  $z_{ff}$ . Carriers are reflected from the rear surface (at least for the LBNL case), so the problem is equivalent to one with the photoionization source with twice the intensity at the center of the field-free substrate with thickness  $2z_{ff}$ . It is sufficient to consider the steady-state solution to the problem, so that Eq. 5 reduces to Laplace's equation except for the  $\delta$ -function at the origin. We recognize this as equivalent to the potential problem in

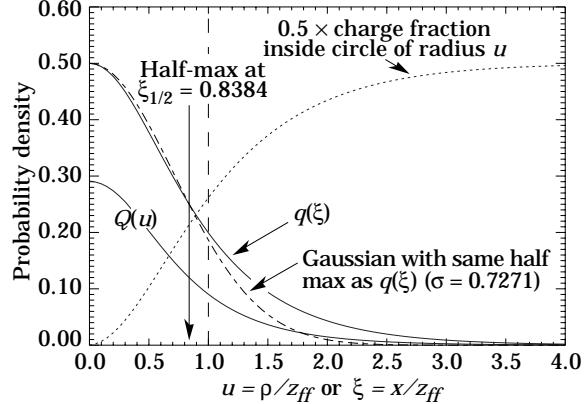


Fig. 3.— The radial charge distribution  $Q(u)$  and marginal distribution  $q(\xi)$  (solid curves). The scaled variables are  $u = \rho/z_{ff}$ , where  $z_{ff}$  is the thickness of the field-free (undepleted) region and  $\rho = \sqrt{x^2 + y^2}$ , and  $\xi = x/z_{ff}$ . With the extension  $q(-\xi) = q(\xi)$ , the variance of  $q(\xi)$  is 1. The distributions are normalized so that  $\int_0^\infty Q(u)2\pi u du = 1$  and  $\int_{-\infty}^\infty q(\xi)d\xi = 1$ .

which a charge is equidistant between two earthed planes at  $z = \pm z_{ff}$  (Hopkinson 1983). In this case the gradient at the plane is normal and gives the electric field, which is in turn proportional to the charge density on the plate. This is a well-studied problem. In particular, Jackson (Jackson 1990) gives two solutions, in his problems 3.17(b) and 3.18(b). For unit total charge on each plane (two negative unit charges at the origin) the charge distribution in the potential problem is exactly equal to the hole distribution at the potential wells in our diffusion problem. We obtain

$$\begin{aligned} Q(u) &= \frac{1}{2\pi} \int_0^\infty dk \frac{k J_0(ku)}{\cosh k} \\ &= -\frac{1}{2} \sum_{m=1}^\infty (-1)^m (2m-1) K_0\left((m-\frac{1}{2})\pi u\right), \end{aligned} \quad (14)$$

where  $J_n$  is the Bessel function regular at the origin,  $K_n$  is the modified Bessel function which is 0 at infinity,  $u = \rho/z_{ff}$ , and  $\rho = \sqrt{x^2 + y^2}$ . This corresponds to Hopkinson's  $z_s = d$  case (Hopkinson 1987).

The integral form converges rapidly for small  $u$ , and only a few terms in the summation given in the second form are necessary for larger arguments. For example, 7-place accuracy is obtained with 8 terms for  $x > 0.5$ , while only 2 terms are nec-

essary for  $x > 2$ . We have therefore used both forms to compute  $Q(u)$ , which is shown in Figure 3. With the function normalized as above, to give a unit charge when integrated over the plane, the amplitude at the origin is a pure number, 0.29156090... (Gradshteyn & Ryzhik (1965) 3.521.2).

The marginal distribution

$$q(\xi) = q(-\xi) = 2 \int_0^\infty Q\left(\sqrt{\xi^2 + \eta^2}\right) d\eta \quad (15)$$

is more relevant to most of our applications; e.g., one calculates the  $x$  moments of a PSF. Here  $\xi = x/z_{ff}$  and  $\eta = y/z_{ff}$ . Half of this function is shown in Figure 3.  $q(0) = 0.5$  and  $\langle \xi^2 \rangle = 1$ . The latter statement is important: the rms in the  $x$  or  $y$  direction is equal to the thickness of the field-free region. This verifies a conjecture by Janesick based on a Monte Carlo simulation (Janesick 1985). The tails of the distribution are much higher than in the Gaussian case. A Gaussian fit to the central region produces  $\sigma = 0.8384z_{ff}$ , not  $z_{ff}$ , and 13% of the charge lies outside a radius of  $2z_{ff}$ .

The behavior is shown in an extreme case ( $z_{ff} = 84 \mu\text{m}$ ) in Figure 4, which shows the projected  $x$  distribution (in  $15 \mu\text{m}$  pixels) for a pinhole image, obtained with a substrate bias of 7.5 V. The width of the solid curve, adjusted visually for a reasonable fit, corresponds to  $z_{ff} = 90 \mu\text{m}$ . The difference is easily consistent with our uncertainty in  $z_J$  and other parameters.

The analysis of Section 2 can also be applied to normal thinned n-channel CCDs, although greater caution must be taken because the dimensions of the sensitive region are not large compared with the pixel size. In such cases there is no substrate bias, but typically  $V_J \approx 20$  V. A one-dimensional calculation indicates that the thickness of the depleted region ranges from 8 to  $18 \mu\text{m}$  as the resistivity of the material is varied from 20 to  $100 \Omega\text{-cm}$ . In general the field does not reach the back surface, and  $z_{ff}$  can be  $\gtrsim 10 \mu\text{m}$ .

This section extends and substantially corrects the discussion of Holland et al. (1997).

## 6. Resolution if diffusion in field-free and depleted regions are comparable

What if we are dealing with a partially depleted CCD in which neither diffusion in the field-free region or diffusion in the depleted region dominates the PSF? We have already observed that all charges with the same collection time contribute to the same (Gaussian) distribution. In this case there are two processes, diffusion in a region with  $E = 0$ , and diffusion of charges drifting under the influence of an electric field in the  $z$  direction. In the second case we have ignored longitudinal diffusion, which dominates near the depletion boundary, and our expression for  $\sigma_d$  is divergent.

Suppose we divide the substrate into two regions, with the boundary just inside the depleted region. In the first region we neglect the electric field, and in the second longitudinal diffusion. In both cases we overestimate the transit time, and hence the resolution contribution. However, if we choose the boundary which gives the smallest sum of the variances, we will have found the minimum combined resolution, and thus the variance closest to reality.

This procedure is illustrated in Figure 5 for a case of experimental interest. At this substrate bias (15.4 V) the substrate is not fully depleted; this will occur at about 17.5 V. We plot the two variances as a function of distance from the depletion boundary. The variance  $\sigma_d^2$  for the depleted region is singular at the boundary, but falls with distance into the region, at first quite rapidly. The field-free variance  $\sigma_{ff}^2$  grows quadratically. The flat minimum of the total variance occurs  $2.3 \mu\text{m}$  from the boundary. While the result is still an overestimate, the algorithm clearly provides a reasonable way to find the combined variance because only one process dominates in most of each region. The PSF itself must be found by convoluting the Gaussian with variance  $\sigma_d^2$  with the non-Gaussian distribution with variance  $\approx (17 \mu\text{m})^2$  from diffusion in the (slightly extended) field-free region.

## 7. Experimental results

Charge diffusion has been characterized by imaging a pinhole mask consisting of small openings etched in a chrome layer on a quartz substrate that was placed directly on a back-illuminated  $2048 \times 2048$  ( $15 \mu\text{m}$ )<sup>2</sup> pixel LBNL CCD. The

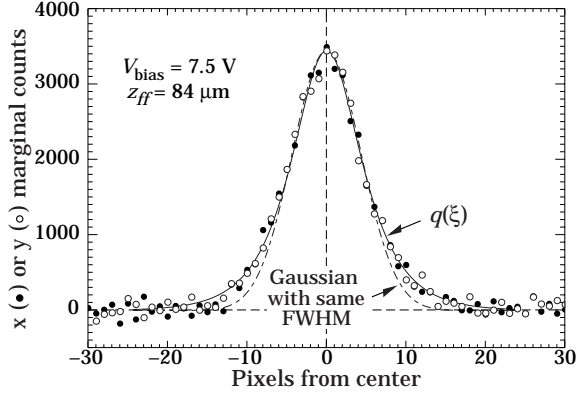


Fig. 4.— Marginal distributions of one pinhole image at a bias of  $V_{\text{sub}} = 7.5$  V. The comparison distribution is from Figure 3.

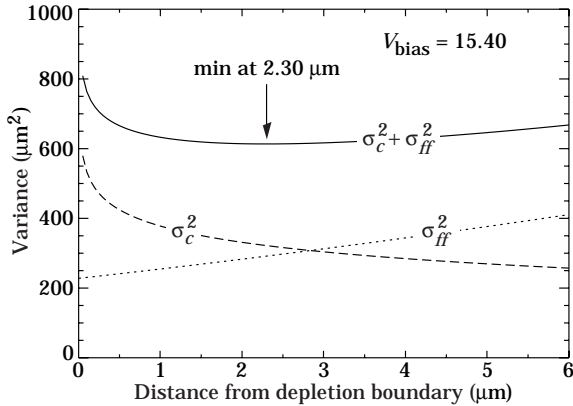


Fig. 5.— Algorithm for finding an upper limit to the combined variance if neither lateral diffusion in the field-free or depleted regions can be neglected.

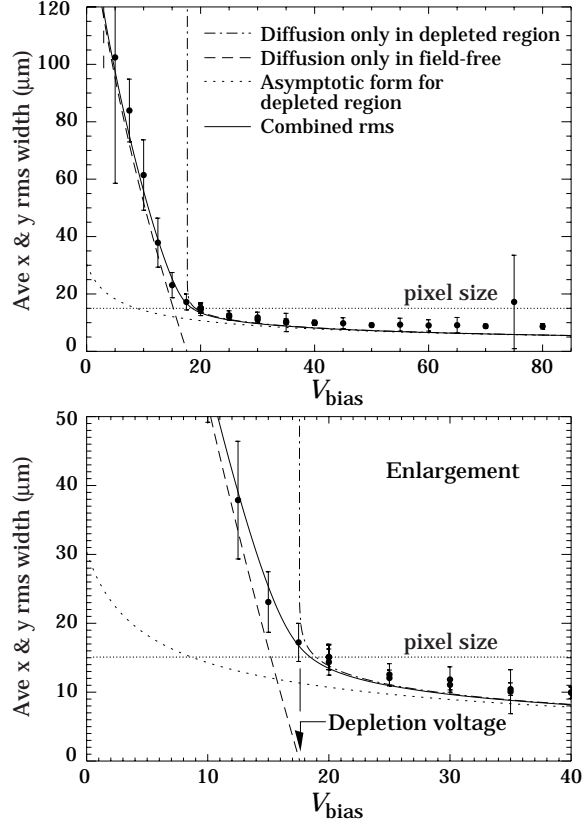


Fig. 6.— Measured standard deviation for a point light source on back of the CCD. In the present analysis, undersampling results in an overestimate of  $\sigma$  for  $\sigma \gtrsim 15$   $\mu\text{m}$ . We compare calculated standard deviations for the overdepletion case, and for underdepletion where  $\sigma$  is dominated by diffusion in the undepleted region. The parameters are chosen using the analysis shown in Figure 7.

8, 4, and 2  $\mu\text{m}$  square holes were arranged as a hexagonal array with 60 pixel spacing.<sup>5</sup> A narrow bandpass filter centered at 400 nm transmitted light which was absorbed within 0.1–0.2  $\mu\text{m}$  from the back surface.

In this preliminary analysis, subframes each containing one almost-centered pinhole image were first surfaced on the basis of edge information. The first two moments of the  $x$  and  $y$  projections were then calculated to obtain the variances. Since the rms image widths varied by a factor of more than ten as the substrate bias voltage was changed, the width of the windows used to calculate the moments was also scaled. When the CCD was totally depleted ( $V_{\text{sub}} \gtrsim 18\text{ V}$ ) the rms width of an image was less than a pixel size.  $\sigma_{\text{pixel}} = 1/\sqrt{12} \times 15\ \mu\text{m}$  was subtracted in quadrature from the measured rms deviation in an attempt to correct for undersampling. Figure 6 shows the results obtained in this way as a function of substrate bias voltage.

To calculate the expected resolution, one needs to know  $V_J$  and  $N_D$ . These can be extracted from the data with the help of Eq. 4. A plot of  $(z_J - z_{ff})^2$  as a function of  $V_{\text{sub}}$  is shown in Figure 7. In the low- $V_{\text{sub}}$  region where field-free diffusion dominates, one should expect a straight line with slope inversely proportional to  $N_D$  and intercept  $V_J$  at  $(z_J - z_{ff})^2 = 0$ . The fit parameters shown in the figure are used to draw the theoretical curves shown in Figure 6, with the aid of Eqns. 11, 12, and 4. The solid curve for the combined resolution is obtained using the algorithm discussed in Sec. 6.

While the theory and data are in reasonable agreement, it is believed that this algorithm did not adequately correct for undersampling when the rms width was substantially less than a pixel size. Improvements in the algorithm have been suggested and will be implemented in the near future.

*Note added in proof:* Using the first form of Eq. 14, Eq. 15 can be integrated with the aid of Gradshteyn & Ryzhik (1965) 6.567.17 and 3.981.3 to obtain

$$q(x) = \frac{1}{2z_{ff} \cosh \pi x / 2x_{ff}}. \quad (16)$$

<sup>5</sup>It would be better to make the spacing incommensurate with pixel spacing and to randomize the positions.

This is the  $q(z/z_{ff})$  shown in Fig. 4 (where  $\xi = z/z_{ff}$ ), which was previously obtained by numerical integration. The corresponding modulation transfer function (MTF) is

$$\text{MTF}(k) = \frac{1}{\sqrt{2\pi} \cosh k}, \quad (17)$$

where  $k$  is the spatial frequency. A future publication will elaborate the consequences of these results.

## REFERENCES

- Burke, B. E. et al. 1991, *IEEE Trans. Elect. Dev.* 38, 1069
- Burke, B. E., Mountain, R. W., Daniels, P. J., Cooper, M. J., & Dolat, V. S. 1994, *IEEE Trans. Nucl. Sci.* 41, 375
- Burke, B. E. et al. 1997, *IEEE Trans. Elect. Dev.* 44(10), 1633
- Gradshteyn, I. S., & Ryzhik, I. M. 1965, *Table of Integrals, Series, and Products*, trans. Alan Jeffrey, Academic Press
- Holland, S. E. et al. 1997, *Proc. 1997 IEEE Workshop on Charge-Coupled-Devices and Advanced Image Sensors*, Bruges, Belgium, June 5–7
- Holland, S. E., et al. 1996, *IEDM Tech. Digest*, 911
- Holland, S. E., Wang, N. W., & Moses, W. W. 1997, *IEEE Trans. Nucl. Sci.* 44, 443–447
- Hopkinson, G. R. 1983, *Nucl. Instrum. Meth.* 216, 423
- Hopkinson, G. R. 1987, *Optical Engineering* 26, 766
- Jackson, J. D. 1975, *Classical Electrodynamics*, 2nd ed., John Wiley & Sons, New York, (1975).
- Janesick, J. et al. 1985, *SPIE* 597, 364
- Kamasz, S. R., Farrier, M. G., & Smith, C. R. 1994, *SPIE* 2172, 76
- McCann, D. M. et al. 1980, *SPIE* 217, 118
- Shockley, W. 1950, *Electrons and Holes in Semiconductors*, D. Van Nostrand, New York, 349

Stover, R. J. et al. 1999, Proc. 4th ESO Workshop on Optical Detectors for Astronomy, Garching, Germany, 13-16 September 1999 (these *Proceedings*)

Tsoi, H. Y., Ellul, J. P., King, M. I., White, J. J., & Bradley, W. C. 1985, IEEE Trans. Elec. Dev. 32, 1525

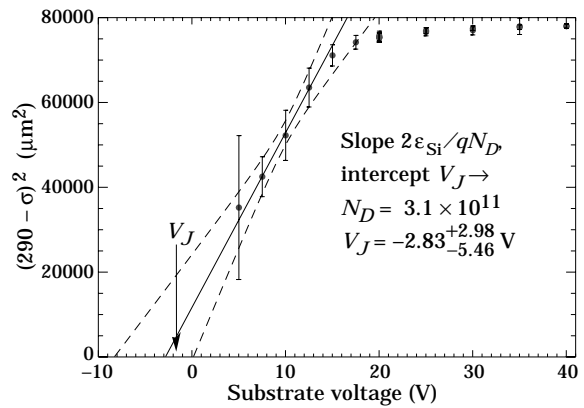


Fig. 7.—  $(z_J - z_{ff})^2$  as a function of  $V_{\text{sub}}$ , as estimated from the observed rms deviation as a function of bias voltage. If diffusion in the undepleted region dominates, this quantity should be linear in the bias voltage, with intercept equal to the effective junction potential  $V_J$  and slope inversely proportional to  $N_D$ , the substrate doping.